

(MS ID: JBC/2014/628123)

Probing the acceptor active site organization of the human recombinant β 1,4-galactosyltransferase 7 and design of xyloside-based inhibitors*

Mineem Saliba¹, Nick Ramalanjaona¹, Sandrine Gulberti¹, Isabelle Bertin-Jung¹, Aline Thomas², Samir Dahbi³, Chrystel Lopin-Bon³, Jean-Claude Jacquinet³, Christelle Breton², Mohamed Ouzzine¹, and Sylvie Fournel-Gigleux¹

¹ UMR 7365 CNRS-Université de Lorraine, Biopôle - Faculté de Médecine, CS 50184, 54505 Vandoeuvre-lès-Nancy Cedex, France

² Univ. Grenoble Alpes, CERMAV, BP 53, 38041 Grenoble Cedex 9, France

³ UMR 7311 CNRS-Institut de Chimie Organique et Analytique, Université d'Orléans-Pôle de Chimie, Rue de Chartres, 45067 Orléans Cedex 02, France

*Running title: *Structure-guided inhibitors of h β 4GalT7*

To whom correspondence should be addressed: Sylvie Fournel-Gigleux, UMR 7365 CNRS-Université de Lorraine, Biopôle - Faculté de Médecine, CS 50184, 54505 Vandoeuvre-lès-Nancy Cedex, France; Tel : +33 (0)3 83 68 54 08; Fax : +33 (0)3 83 68 54 09; e-mail : sylvie.fournel-gigleux@univ-lorraine.fr

Key words: glycosaminoglycan, glycosyltransferase, proteoglycan synthesis, enzyme inhibitor, site-directed mutagenesis, enzyme kinetics

Background: Glycosyltransferase inhibitors have important applications in therapeutics and as chemical biology tools.

Results: The human β 1,4-galactosyltransferase 7 enzyme active site was mapped by modeling, mutagenesis, *in vitro/in cellulo* assays and novel inhibitors were synthesized.

Conclusion: An efficient inhibitor of β 1,4-galactosyltransferase 7 and glycosaminoglycan synthesis was obtained.

Significance: This inhibitory molecule can be exploited to investigate glycosaminoglycan biology and modulate glycosaminoglycan synthesis in therapeutics.

ABSTRACT

Among glycosaminoglycan (GAG) biosynthetic enzymes, the human β 1,4-galactosyltransferase 7 (h β 4GalT7) is characterized by its unique capacity to take over xyloside derivatives linked to a hydrophobic aglycone as substrates and/or inhibitors. This glycosyltransferase is thus a prime target for the development of regulators of GAG synthesis in therapeutics. Here, we report the structure-guided design of h β 4GalT7 inhibitors. By combining molecular modeling, *in vitro* mutagenesis and kinetic measurements, and *in*

Glycosaminoglycans (GAGs) are linear heteropolysaccharide chains covalently attached to

cellulo analysis of GAG anabolism and decorin glycosylation, we mapped the organization of the acceptor binding pocket, in complex with 4-methylumbelliferone-xylose (4-MUX) as prototype substrate. We show that its organization is governed, on one side, by three tyrosine residues, Y194, Y196 and Y199, which create a hydrophobic environment and provide stacking interactions with both xylopyranoside and aglycone rings. On the opposite side, a hydrogen-bond network is established between the charged amino acids D228, D229 and R226, and the hydroxyl groups of xylose. We identified two key structural features *i.e.* the strategic position of Y194 forming stacking interactions with the aglycone, and the hydrogen bond between H195 nitrogen-backbone and the carbonyl group of the coumarinyl molecule to develop a tight binder of h β 4GalT7. This led to the synthesis of 4-deoxy-4-fluoro-xylose linked to 4-MU that inhibited h β 4GalT7 activity *in vitro* with a K_i ten-times lower than the K_m value and efficiently impaired GAG synthesis in a cell assay. This study provides a valuable probe for the investigation of GAG biology and opens avenues towards the development of bioactive compounds to correct GAG synthesis disorders implicated in different types of malignancies.

the core protein of a variety of proteoglycans (PGs). Owing to their high structural diversity and their

anionic characteristics, GAGs interact with a network of cellular and extracellular mediators including cytokines and chemokines, enzymes and enzyme inhibitors, matrix proteins and membrane receptors (1). There is currently great emphasis on the crucial roles of GAGs in numerous physiological events including cell differentiation, proliferation and migration (2), and its pathological aspects, such as tumor formation, progression and metastasis (3). Furthermore, since PGs are ubiquitously expressed in extracellular matrices and on cell surfaces of virtually every tissue, they are also involved in the normal and pathological functions of the cardiovascular and osteo-articular system (4), in amyloid disorders (5) and in axonal de- and regeneration (6). GAG biosynthesis is initiated by the formation of a tetrasaccharide linkage region (GlcA β 1-3Gal β 1-3Gal β 1-4Xyl β 1-O-) covalently linked to serine residues of the PG core protein (7). This tetrasaccharide acts as a primer for the elongation of major GAG chains *i.e.* chondroitin-/dermatan-sulfate (CS/DS) or heparin/heparan-sulfate (HS), which polymerization involves the coordinated activities of CS-synthases (CSS) and HS-synthases (exostosins, EXT), respectively (8, 9). Mature GAG chains are finally produced by the modifications of their constitutive disaccharide units catalyzed by epimerases and sulfotransferases which considerably increase their structural and functional diversity (10, 11).

The human xylosylprotein β 1,4-galactosyl transferase, (EC 2.4.1.1337, h β 4GalT7) catalyses the transfer of the first Gal residue of the tetrasaccharide linkage from the activated sugar UDP-galactose (UDP-Gal) onto Xyl residues attached to the PG core protein (12). Since all GAGs share the same stem core tetrasaccharide, β 4GalT7 is a central enzyme in GAG biosynthesis. Indeed, h β 4GalT7 mutations have been associated with a rare genetic condition, the progeroid form of Ehlers-Danlos syndrome (EDS), a group of connective tissue disorders, characterized by a major deficiency in PG synthesis. As a consequence of GAG defect, EDS patients exhibit motor development delay, and musculoskeletal malformations, hypermobile joints and wound healing defaults (13). Patients gene sequencing revealed the presence of missense mutations leading to L206P, A186D (14, 15) and R270C substitutions (16) in the catalytic domain, resulting in a partially or totally inactive enzyme. Recently, we showed that R270C replacement reduced affinity towards xyloside acceptor and strongly affected GAG chains formation in β 4GalT7-deficient CHOpgsB-618 cells (17). There is currently no effective therapy for treating EDS patients.

Interestingly, the biosynthesis of GAGs can be

manipulated by simple xylosides carrying a hydrophobic aglycone, which act as substrates and/or inhibitors of h β 4GalT7. Xyloside analogs have been shown to efficiently induce GAG synthesis bypassing the natural Xyl-substituted core protein of PGs for several decades (18, 19). The xyloside-primed GAG chains are usually excreted and show interesting biological functions such as activation of fibroblast growth factor (FGF)-signaling (20, 21), antithrombotic (22), tissue regenerating (23), anti-angiogenic (24) and anti-proliferative properties (25, 26). In addition, several groups have synthesized series of xyloside analogs as potential inhibitors of GAG synthesis. Such compounds would represent highly valuable chemical biology tools to probe the functions of GAGs in cell systems and model organisms and as a starting point towards the development of pharmaceuticals, in particular anti-tumor agents. Recently, Garud *et al.* (27) and Tsuzuki *et al.* (28) used click chemistry to generate libraries of 4-deoxy-4-fluoro-triazole analogs comprising a set of hydrophobic molecules appended to the anomeric carbon of the xyloside. Siegbahn *et al.* (29, 30) developed a collection of naphthyl- and benzyl-xylosides substituted on different positions of the Xyl moiety. These studies led to the discovery of promising xyloside-derived inhibitors of GAG synthesis when screened in cell models.

However, until recently, the development of substrates and inhibitors of β 4GalT7 has been mostly limited to the synthesis of libraries of analog compounds and their testing in cell assays. Towards the rational design of h β 4GalT7 inhibitors, we have been involved in structure-activity relationship studies of the recombinant human enzyme for several years and identified critical active site amino acids implicated in catalysis and/or substrate binding (17, 31, 32). We previously investigated the importance of conserved ¹⁶³DVD¹⁶⁵ and ²²¹FWGWRGEDDE²³⁰ motifs in the organization of the catalytic domain. Our data have highlighted the crucial role of W224 in substrate recognition and suggested a catalytic role for D228 (31). These findings were in accordance with the structural data from the recently solved crystal structure of the catalytic domain of *Drosophila melanogaster* d β 4GalT7 (33) and that of the human enzyme (34).

In the current study, we developed a structure-guided approach for the design of xyloside inhibitors of h β 4GalT7 that were tested on its galactosyltransferase activity *in vitro* and on GAG biosynthesis in cell assays. We explored the organization of the acceptor binding pocket, specifically probing the functional and structural contribution of a set of residues located in the vicinity of the catalytic center, and highlighted the

crucial role of three tyrosine residues *i.e.* Y194, Y196 and Y199 in the architecture of the acceptor substrate binding site and the creation of a hydrophobic environment. Based on these and previous findings, we synthesized compounds that incorporate critical structural elements both on the xylopyranoside and on the aglycone moieties to tightly bind the acceptor site of h β 4GalT7. This work revealed that the 4-deoxy-4-fluoro-Xyl linked to 4-methylumbelliferone (4-MU) strongly inhibited h β 4GalT7 activity *in vitro* and efficiently impaired GAG synthesis in a cell context. Such compound will be a valuable tool for the exploration of GAG and PG synthesis and opens avenues towards the development of bioactive oligosaccharide structures for GAG biosynthesis regulation in a number of diseases implicating disorders of GAG synthesis.

EXPERIMENTAL PROCEDURES

Chemicals and Reagents – 4-Methylumbelliferyl- β -D-xylopyranoside (4-MUX), UDP- α -D-Gal (UDP-Gal) and anti-goat IgG (whole molecule)-peroxidase conjugated antibody were provided from Sigma Aldrich. Anti-myc antibodies were from Invitrogen and anti-mouse IgG-peroxidase antibodies were purchased from Cell Signaling whereas anti-decorin antibodies were from R&D systems. Na₂[S³⁵]SO₄ was from PerkinElmer Life Sciences. Cell culture medium was purchased from Life Technologies and restriction enzymes, T4 DNA ligase and peptide *N*-glycosidase F (PNGase F) from New England Biolabs. The eukaryotic expression vector pcDNA3.1(+) and competent One Shot[®] Top 10 *Escherichia coli* (*E. coli*) cells were provided from Invitrogen and the bacterial expression vector pET-41a(+) and *E. coli* BL21(DE3) cells were from Novagen-EMD Chemicals. The QuikChange site-directed mutagenesis kit was from Stratagene and the transfection agent ExGen 500 from Euromedex.

Chemical Synthesis – Naphthyl-4-deoxy- β -D-xylopyranoside (4H-Xyl-NP) (29) was obtained after protection of the 2,3 position of naphthyl- β -D-xylopyranoside by isopropylidene acetal followed by radical deoxygenation and deprotection. 4-Methylumbelliferyl-4-deoxy- β -D-xylopyranoside (4H-Xyl-MU) and 4-methylumbelliferyl-4-fluoro- β -D-xylopyranoside (4F-Xyl-MU) were synthesized from the reported starting material 4-methylumbelliferyl-2,3-di-*O*-benzoyl- β -D-xylopyranoside (35) by radical deoxygenation or stereocontrolled 4-fluorination followed by final deprotection (data not shown).

Molecular modeling of h β 4GalT7 active site in the presence of 4-MUX and UDP-Gal – The crystal structure of h β 4GalT7 bound to UDP and to the manganese ion (PDB ID: 4IRQ) was used as template (34). The crystal structure of d β 4GalT7

(PDB ID: 4M4K), an inactive mutant (D211N) of d β 4GalT7 in complex with UDP-Gal and xylobiose was superposed to the human enzyme structure, which was straightforward considering their strong sequence similarity (58% overall identity). Due to crystallization conditions, a Tris molecule is bound within the active-site of the h β 4GalT7. When retrieved, it frees space within the cavity that can thus accommodate the Gal moiety. The coordinates of the Gal molecule from the d β 4GalT7 complex were merged to the UDP moiety of h β 4GalT7. This did not generate any steric clash within the active site. The resulting complex was then prepared using the Protein Preparation Wizard tool of the Schrödinger Suite (<http://www.schrodinger.com>, Schrödinger LLC, New York), with default settings (36). All the water molecules were retrieved, except the one that coordinates the manganese ion. The hydrogen atoms were added to the protein and the ligand, ascribing a pH of 7.0. The histidine residues were treated as neutral. The selection of the histidine enantiomers and the orientation of the asparagine and glutamine side-chains were performed so as to maximize the hydrogen bond network. The partial atomic charges derived from the OPLS-2005 force field (37) were assigned to all ligand and protein atoms. Finally, an all-atom energy minimization with a 0.3 Å heavy-atom root-mean-square deviation (RMSD) criteria for termination was performed using the Impref module of Impact and OPLS-2005 (38). The 4-MUX ligand was prepared using the ligprep module (Schrödinger Release 2014-22014). The docking program Glide was used in Standard Precision mode, with OPLS-2005, to run rigid-receptor docking calculations (39, 40). The shape and physico-chemical properties of the binding site were mapped onto a cubic grid with dimensions of 20 Å³ centered on the xylobiose. During the docking calculations, the parameters for van der Waals radii were scaled by 0.80 for receptor atoms with partial charges less than 0.15e. Ring conformational sampling was not allowed to maintain the ⁴C₁ conformation of the Xyl ring, and no constraint was introduced. A maximum of 100 poses were retained and ranked according to the GlideScore scoring function. The best-docked pose of the 4-MUX ligand showed a RMSD on the Xyl ring heavy atoms of 0.5 Å with the crystallographic xylobiose ligand, thus validating the docking protocol able to recover the position of this moiety.

Expression vector construction – The h β 4GalT7 sequence (GenBank[®] nucleotide sequence accession number NM_007255) was cloned by PCR amplification from a placenta cDNA library (Clontech), as previously described (41). For bacterial expression, a truncated form of h β 4GalT7 was expressed as a fusion protein with glutathione-

S-transferase (GST). The sequence lacking the codons of the first 60 N-terminal amino acids was amplified from the full-length cDNA and subcloned into *Nco*I and *Not*I sites of pET-41a(+) to produce the plasmid pET- β 4GalT7 (31). For the heterologous expression of h β 4GalT7 in mammalian cell lines, the full-length cDNA sequence was modified by PCR at the 5' end to include a *Kpn*I site and a Kozak consensus sequence, and at the 3' end to include a sequence encoding a myc tag and an *Xba*I site to be then subcloned into the *Kpn*I-*Xba*I sites of the eukaryotic expression vector pcDNA3.1(+) to produce pcDNA- β 4GalT7 as previously described (31). Mutations were constructed using QuikChange site-directed mutagenesis kit, employing pcDNA- β 4GalT7 or pET- β 4GalT7 as template. Sense and antisense primers are listed in supplemental Table 1. Mutants were systematically checked by double strand sequencing. The human decorin cDNA sequence (GenBank[®] accession number NM_001920.3) was cloned by PCR amplification from a placenta cDNA library (Clontech). For heterologous expression in eukaryotic cells, the full-length cDNA sequence was modified by PCR to include an *Afl*III site, a Kozak consensus sequence at the 5' end, a sequence encoding a His₅ tag, and an *Xho*I site at the 3' end. This sequence was subcloned into pcDNA3.1(+) to produce pcDNA-decorinHis as previously described (31).

Expression and purification of the soluble form of h β 4GalT7 – A single colony of *E. coli* BL21(DE3) cells transformed with the pET- β 4GalT7 plasmid was cultured overnight at 37 °C in a Luria broth (LB) medium containing 50 μ g/mL kanamycin. The overnight culture was transferred into fresh LB medium (1:100 dilution), supplemented with 50 μ g/mL kanamycin and incubated at 37 °C until the OD₆₀₀ value reached 0.6-0.8. Expression of h β 4GalT7 was induced by addition of 1 mM isopropyl- β -D-thiogalactopyranoside (IPTG) to the cell suspension, that was then incubated overnight at 20 °C under continuous shaking (200 rpm). The bacterial cells were then harvested by centrifugation at 7,000 \times g for 10 min at 4 °C. The pellet was resuspended in Lysis buffer (50 mM sodium phosphate, 1 mM phenylmethylsulfonyl fluoride, 1 mM EDTA, and 5% (v/v) glycerol, pH 7.4) supplemented with protease inhibitor cocktail tablets (1 tablet /12 mL; Roche Diagnostics) and Benzonase[®] Nuclease (250 units/10 mL, Sigma Aldrich). The suspended cells were then sonicated for 8 cycles of 30 sec, at 30% power (Badelin Sonoplus GM70) with a 20 sec-interval on ice between each cycle. Soluble proteins were collected from the supernatant after centrifugation for 25 min at 12,000 \times g and clarification by filtration (0.2 μ M

Supor[®] Membrane; PALL-Life Science). 10 mL of clarified extracts were applied onto a 1 mL a Glutathione Sepharose High Performance column (GSTrap HP; GE Healthcare) connected to an AKTA prime plus instrument (GE Healthcare). Protein were eluted as 1 mL-fractions using 50 mM Tris-HCl, pH 8.0 containing 10 mM reduced glutathione buffer. Protein purity of the eluted fractions was evaluated by 12% (w/v) SDS-PAGE analysis, followed by staining with Coomassie Brilliant Blue. Fractions containing the pure protein were used to determine the kinetic parameters of the enzyme. The same procedure was used for purification of the mutants. Protein concentration was measured using Quant-iT[™] assay kit and Qubit[™] spectrofluorimeter.

Determination of the in vitro kinetic parameters of h β 4GalT7 – The kinetic parameters k_{cat} and K_m towards 4-MUX and UDP-Gal were determined as described (31). Briefly, 0.2 μ g of purified wild-type or mutated GST-h β 4GalT7 were incubated for 30 min at 37 °C in a 100 mM sodium cacodylate buffer pH 7.0, 10 mM MnCl₂, with concentrations from 0 to 5 mM 4-MUX in the presence of fixed 1 mM UDP-Gal to determine the apparent K_m towards 4-MUX, and with concentrations from 0 to 5 mM UDP-Gal in the presence of fixed 5 mM 4-MUX to determine the apparent K_m towards UDP-Gal. The incubation mixture was then centrifuged at 10,000 \times g for 10 min at 4 °C. The supernatant was analyzed by high performance liquid chromatography (HPLC) with a reverse phase C18 column (xBridge, 4.6 x 150 mm, 5 μ m, Waters) using a Waters equipment (Alliance Waters e2695) coupled to a UV detector (Shimadzu SPD-10A). Kinetic parameters were determined by nonlinear least squares regression analysis of the data fitted to Michaelis-Menten rate equation using the curve-fitter program of Sigmaplot 9.0 (Erkraft, Germany).

In vitro competition assays of h β 4GalT7 activity by C4-modified xylosides – The *in vitro* inhibition assays of the wild-type GST-h β 4GalT7 were carried out using 0.2 μ g of purified protein incubated for 30 min at 37 °C in a 100 mM sodium cacodylate buffer pH 7.0, 10 mM MnCl₂, with 0.5 mM 4-MUX and 1 mM UDP-Gal, in the presence of concentrations from 0 to 5 mM of either 4H-Xyl-NP, 4H-Xyl-MU, or 4F-Xyl-MU. Quantification of the reaction product was carried out by HPLC, as described above. The enzyme activities were reported as function of the logarithmic values of inhibitor concentration. IC₅₀ values were determined by fitting the experimental dose-response curves using the curve-fitter program of Sigmaplot 9.0 (Erkraft, Germany). K_i values were calculated from IC₅₀ values according to the Cheng-Prusoff's equation (42, 43).

In cellulo analysis of GAG chains biosynthesis by $\text{Na}_2[^{35}\text{SO}_4]$ incorporation – GAG chains biosynthesis using 4-MUX as primer substrate was determined with CHOpgsB-618 cells (American Type Culture Collection). Cells were cultured in Dulbecco's modified Eagle's medium-F12 (DMEM/F12) (1:1), supplemented with 10% fetal bovine serum (FBS, Dutscher), penicillin (100 units/ml)/ streptomycin (100 mg/ml), and 1 mM glutamine, then transfected with the wild-type or the mutant pcDNA- β 4GalT7-myc plasmid or with the empty pcDNA3.1 vector at 70% cell confluency. Transfected cells were then incubated in a low sulfate medium (Fisher) supplemented with 10 $\mu\text{Ci/mL}$ $\text{Na}_2[^{35}\text{SO}_4]$ in the presence of 0.5 or 10 μM 4-MUX for 16 h. For GAG chains isolation 1 mL culture medium was applied to a G-50 column (GE Healthcare) to separate radiolabeled GAG chains from the non-incorporated $\text{Na}_2[^{35}\text{SO}_4]$ and radiolabeling was quantified by scintillation counting. In parallel, h β 4GalT7 expression level was checked by western blotting using a primary anti-myc (1/5000) and a secondary anti-mouse antibody (1/10000). To test the inhibitory potency of C4-modified xylosides, the molecules were added at 0 to 100 μM concentration together with 4-MUX (5 μM) for 16 h prior to isolation and quantification of radiolabeled GAGs. To test the cytotoxicity of xyloside inhibitors in CHOpgsB-618 cells expressing the wild-type h β 4GalT7, cells were seeded at 150,000 cells/well in 12-well plates, and incubated for 48 h at 37 °C in the presence of 0 to 400 μM of inhibitor, or 4-MUX as a control. The ratio of viable cells upon the total number of cells was determined using the cell counter TC20 (BioRad) in the presence of a vital marker (Trypan blue).

In cellulo analysis of decorin core protein glycosylation – CHOpgs-B618 cells stably transfected with pcDNA-decorinHis encoding the human decorin core protein (31, 44) were transiently transfected with pcDNA3.1 or with recombinant vector encoding either the wild-type or mutated h β 4GalT7-myc as described above. 48 Hours following transfection, the cell medium was collected, concentrated by centrifugation at 4 °C for 15 min at 3000 \times g, using the Amicon Ultracell 30 MWCO concentrating system (Merck Millipore, Germany) and submitted to SDS-PAGE (25 μg protein per well). The glycosylation level of the decorin core protein was monitored by immunoblot using a 1/5,000 dilution of primary polyclonal anti-human decorin antibody (VWR) and a 1/10,000 dilution of secondary anti-goat antibody coupled to horseradish peroxidase (Sigma Aldrich), then quantified using ImageJ software. Briefly, the level of decorin glycosylation was expressed as relative

band intensity by normalizing the band intensity value for the glycosylated form upon the total intensity value for the bands corresponding to the glycosylated and non-glycosylated forms of decorin core protein. The expression level of the decorin core protein in pcDNA3.1-transfected cells was used as negative control and served as a loading control. On the other hand, the level of glycosylated decorin in cells expressing the wild-type h β 4GalT7 was used as positive control for decorin glycosylation.

RESULTS

Molecular modeling of the h β 4GalT7 acceptor binding site – In the present study, we aimed to identify amino acids important for the structural organization of the h β 4GalT7 acceptor substrate binding site. We took advantage of the recent crystal structure of h β 4GalT7 in complex with UDP (34) to build a molecular model of this enzyme in complex with both the sugar donor UDP-Gal and the acceptor 4-MUX (Fig. 1A). The modeled structure is in a closed conformation, considered to be the catalytically competent form, and the hydrogen bond network around the UDP moiety is fully conserved. We first examined the position of a series of tyrosine residues *i.e.* Y194, Y196 and Y199 that were suggested to be involved in the binding of xylobiose in the d β 4GalT7 structure (33). Our computational analysis indicates that Y194 stabilizes both the donor and acceptor substrates location by establishing a hydrogen bond with a β -phosphate oxygen of UDP-Gal and a π -stacking interaction with the 4-methylumbelliferyl moiety, respectively (Fig. 1A). Residue Y196 is not hydrogen-bonded to the substrates but to the side-chain of residue D229, allowing its second carboxylic oxygen to be suitably oriented to form a hydrogen bond with the O2 atom of Xyl. The spatial orientation of Y199 inside the substrate binding pocket allows the formation of a hydrogen bond between its side-chain hydroxyl and the O2 atom of the Gal moiety of UDP-Gal. Altogether, residues Y194, Y196 and Y199 form a strongly hydrophobic cluster that is required for correct binding of the substrates.

Analysis of the position of H195, a conserved amino acid located between the two active site Y194 and Y196 residues, shows no hydrogen bond involving its side-chain. However, the backbone nitrogen atom of this residue is hydrogen-bonded with the CO group of 4-MUX (Fig. 1A). As illustrated in figure 1B, R226 is located on the surface of the acceptor binding site contributing to an amphipathic entry door with the aromatic residues. In our model, there is no hydrogen bond involving the side-chain of R226. Instead, its

backbone nitrogen atom is hydrogen-bonded with the O3 atom of the Xyl moiety of 4-MUX (Fig. 1A).

The structural impact of R270 on enzyme activity, in the context of EDS was also addressed. The model structure of h β 4GalT7 reveals that R270 belongs to the flexible loop [261-284] that moves upon donor substrate binding, thus creating the acceptor substrate binding site (Fig. 1A). This conformational change leads to the closed and catalytically competent conformation of the active site. However, the crystal structure of the human enzyme (34), as well as our own model in complex with both the donor and acceptor substrates do not highlight specific interactions established by this residue, although its close location to the surface of the active site has to be underlined (Fig. 1B).

Kinetic properties of the human recombinant h β 4GalT7 mutants expressed in E. coli – To assess the functional importance of the residues of the acceptor binding site highlighted by our model, we carried out point mutagenesis and analyzed the consequences of conservative and non-conservative mutations on the kinetic parameters of h β 4GalT7 expressed and purified from recombinant *E. coli* cells. The wild-type enzyme and engineered mutants were produced as truncated fusion proteins lacking the 60 N-terminal amino acids (including the transmembrane domain and part of the stem region) linked to GST and purified by affinity chromatography (data not shown). This led to 1.0 to 2.5 mg of pure protein per liter of culture for wild-type and mutant h β 4GalT7. Kinetic assays were performed using 4-MUX as acceptor substrate, which allowed quantification of the transfer reaction product by UV-detection coupled to HPLC. The k_{cat} and K_m values of the wild-type enzyme towards UDP-Gal and 4-MUX shown in table 1 were in agreement with previous work (17, 31).

Substitution of Y194 by alanine led to an inactive enzyme, and its conservative substitution by phenylalanine did not restore the galactosyltransferase activity of h β 4GalT7 (Table 1), indicating a critical role of this residue and, importantly, of the hydroxyl group of the tyrosine side-chain. The mutation of Y196 to alanine totally abolished enzyme activity whereas replacement of this residue by phenylalanine led to a slightly active enzyme. The Y196F mutation did not impair enzyme affinity towards the donor substrate to a major extent but this mutant presented a lower affinity towards 4-MUX with a K_m value about three-fold that of the wild-type enzyme (Table 1). As observed in the case of Y194 and Y196, the non-conservative mutation Y199A led to a total loss of enzyme activity. However, similarly with what was observed for Y196, substitution of Y199 by phenylalanine led to an active h β 4GalT7 enzyme

with K_m values towards UDP-Gal and 4-MUX and k_{cat} value only weakly affected compared to the wild-type enzyme. These data suggest that the aromatic ring of phenylalanine at position 199 is sufficient to support xyloside binding and activity.

Substitution of H195 by alanine, glutamine or arginine was carried out. The K_m values of all three mutants towards UDP-Gal and 4-MUX were mostly comparable to those of the wild-type enzyme, indicating that these mutations had no major effect upon h β 4GalT7 affinity towards its substrates. Moreover, the substitutions at position 195 did not affect the rate of reaction transfer, as indicated by the k_{cat} values that were essentially unchanged (Table 1). Altogether, these results indicate that the side-chain of H195 does not play a critical role in xyloside binding and h β 4GalT7 catalytic activity. Substitution of R226 by alanine or lysine did not impair the affinity towards the substrates with K_m values for UDP-Gal and 4-MUX, that were in the same range to that of the wild-type enzyme, and produced a moderate decrease (about two-fold) of the catalytic constant value (Table 1).

The R270 residue is mutated to cysteine in the progeroid form of EDS syndrome, and we previously showed that this mutation led to a significant decrease in h β 4GalT7 activity, mainly due to a reduced affinity towards 4-MUX (about ten-fold, see ref. 17). In order to ascertain the contribution of this residue in h β 4GalT7 activity and xyloside binding, we performed kinetic assays following the conservative R270K and non-conservative R270A mutations. The k_{cat} values for both mutants were about two-times lower than that found for the wild-type enzyme and the K_m value towards UDP-Gal was almost unaffected (Table 1).

Effect of Y194, Y196, Y199, H195, R226 and R270 mutations on the galactosyltransferase activity of h β 4GalT7 towards 4-MUX in cellulo – To check the importance of the selected residues onto h β 4GalT7 function in a cellular context, we designed an experimental procedure involving CHOpgsB-618 cells transfected with h β 4GalT7 cDNA encoding either the wild-type or the mutant enzymes fused to a myc-tag sequence at their C-terminal end, as described in *Experimental Procedures*. CHOpgsB-618 cells expressing the recombinant enzymes were tested for *in cellulo* galactosyltransferase activity in the absence or in the presence of 4-MUX as exogenous acceptor substrate. The expression level of enzymes was checked by immunoblot analysis using ImageJ software. As shown in figure 2, an additional upper band at ~39kDa was observed (Fig. 2, insert). This ~39kDa band can be attributed to the N-glycosylated form of the enzyme as it disappears upon PNGase F digestion (Fig. 2, insert, *left panel*). Both bands were taken into account to quantify the

total enzyme expression level. The results indicate that all mutants considered in these experiments were expressed at a similar level to that of the wild-type protein (Fig. 2, insert, *right panel*). As shown in figure 2, the GAG synthesis level in cells expressing wild-type h β 4GalT7 was about 7- and 9.5-fold higher in the presence of 4-MUX at 5 and 10 μ M concentration, respectively, than in the absence of acceptor substrate, indicating that CHOpgsB-618 cells expressing h β 4GalT7 are able to prime efficiently GAG chains synthesis from 4-MUX, in agreement with previous studies (17, 31).

As expected, cells expressing either Y194A or Y194F mutant in the presence of 4-MUX showed GAG synthesis levels comparable to those obtained with cells transfected with empty vector (Fig. 2). These *in cellulo* assays confirm that any mutation affecting the Y194 position leads to a total loss of h β 4GalT7 activity. Substitution of Y196 to alanine dramatically reduced the GAG synthesis rate whose level in the presence of 4-MUX was comparable to that obtained with cells transfected with empty vector. This is consistent with the loss of enzymatic activity observed in the *in vitro* assays (Table 1). By contrast, the conservative mutation Y196F allowed GAG chain priming from 4-MUX. However, the GAG expression level reached with this mutant was about 2 to 3-fold lower than that of the wild-type enzyme, at 4-MUX at 5 and 10 μ M concentrations, respectively (Fig. 2). This result is consistent with the drastic decrease of the k_{cat}/K_m value towards 4-MUX found for the purified Y196F mutant. Comparable results were obtained with cells expressing h β 4GalT7 whose sequence is mutated on the Y199 position. Indeed, cells expressing Y199A mutant were unable to synthesize GAG chains from 4-MUX, whereas cells expressing Y199F showed GAG chains synthesis at a level about half of that observed with cells expressing wild-type enzyme (Fig. 2). These results are in line with the reduced efficiency exhibited *in vitro* by the enzyme substituted on the Y199 position (Table 1). Altogether, these results demonstrate that both conservative and non-conservative mutations affecting either Y194, Y196 or Y199 position significantly impaired GAG chains biosynthesis in a cellular context, in line with *in vitro* data (Table 1).

In the presence of 4-MUX, the GAG synthesis rate in cells expressing H195A, H195Q and H195R mutants was moderately reduced, *i.e.* 10 to 15% lower than that of cells expressing the wild-type enzyme (Fig. 2). These results indicate that the side-chain of this residue does not influence the galactosyltransferase activity of h β 4GalT7 in the context of 4-MUX-primed GAG chains in eukaryotic cells, corroborating the findings that none of the mutations of H195 did significantly

affect *in vitro* activity (Table 1). The level of [$^{35}\text{SO}_4^{2-}$] incorporation in the presence of 4-MUX in cells expressing R226A was about 2-times lower than that of the wild-type enzyme (Fig. 2). In addition, replacement of R226 by lysine slightly increased the GAG expression level compared to alanine substitution, reaching about 60% that obtained with the wild-type, at 5 and 10 μ M 4-MUX concentration. Corroborating *in vitro* kinetic parameters, these cellular assays indicate that modification of the side-chain of R226 produces minor effects on galactosyltransferase activity.

We finally examined the impact of mutations of the R270 residue upon GAG synthesis in eukaryotic cells. We observed that the GAG synthesis rate in cells expressing R270A mutant was about 55% lower than that of the wild-type enzyme, at 5 and 10 μ M 4-MUX concentration (Fig. 2). The GAG synthesis level of the conservative mutant R270K was also about two-fold reduced compared to the wild-type (Fig. 2). These results confirm that mutations of R270 significantly affect the capacity of h β 4GalT7 to synthesize GAG chains from 4-MUX in a cellular context.

Effect of Y194, Y196, Y199, H195, R226 and R270 mutations on the ability of h β 4GalT7 to initiate the glycosylation of the decorin PG in cellulo – We next determined whether the mutations would affect GAG chain formation on the core protein of decorin, used as a model PG (31). To this aim, CHOpgsB-618 cells were engineered to stably express the recombinant human decorin, and were transiently transfected with a pcDNA3.1 vector encoding the wild-type or the mutant forms of h β 4GalT7. This allowed monitoring GAG substitution of the secreted PG by western blot analysis (Fig. 3, insert, *left and right panels*). The rates of the decorin PG glycosylation in cells expressing the wild-type or mutant h β 4GalT7 were determined as described in *Experimental Procedures*, then reported onto the histogram (Fig. 3). Results showed that non-conservative mutations of the tyrosine residues at position 194, 196 and 199 as well as mutations of Y194 and Y196 to phenylalanine fully abolished the glycosylation of decorin (Fig. 3). These data were consistent with the drop of GAG chains primed from 4-MUX in cells expressing h β 4GalT7 mutated at these positions (Fig. 2). However, the substitution of Y196 to phenylalanine induced a more dramatic effect on the glycosylation of decorin than on the *in vitro* or *in cellulo* activity towards 4-MUX. Furthermore, results shown in figure 3 indicate that the conservative mutation Y199F allowed to recover up to 70% of the decorin glycosylation level compared to cells expressing the wild-type h β 4GalT7.

We also assessed the role of the H195 residue in

the glycosylation process of decorin. The results shown in figure 3 indicate that none of the mutations H195A, H195Q or H195R significantly affected the level of decorin glycosylation. These data are consistent with the results obtained on the *in vitro* and *in cellulo* activity of the enzyme towards 4-MUX. Together, mutagenesis experiments indicate that modification of the amino acid side chain at position 195 did not greatly affect xyloside binding and galactosyltransferase activity of h β 4GalT7. Investigation of the effect of R226 mutation upon the ability of CHOpgsB-618 cells to glycosylate decorin showed that the glycosylation level reached with cells expressing R226A or R226K was about 65% of that obtained with cells expressing the wild-type enzyme. These results were consistent with the *in vitro* and *in cellulo* GAG chain synthesis assays (Fig. 3).

Since we aimed to better understand the molecular basis of the EDS syndrome, it was important to further investigate the impact of mutations affecting the R270 position upon the decorin glycosylation. The decorin glycosylation level reached with cells expressing either R270A or R270K mutant was about half of that obtained with cells expressing the wild-type h β 4GalT7, consistent with *in vitro* and *in cellulo* galactosyltransferase assays (Fig. 3).

Xyloside inhibitors design and in vitro and in cellulo competition assays – We next took advantage of the knowledge gained from our investigation of the organization of the acceptor substrate binding site to synthesize and test xyloside analogs as potential inhibitors of h β 4GalT7. To this end, *in vitro* competition assays were performed as described in *Experimental Procedures*. The specific activity as a function of the logarithm values of the inhibitor concentrations are reported in figure 4B and data fitted to the logistic equation provided IC₅₀ values reported in Table 2.

Since the C4-position is critical for both binding and transfer of the Gal residue from UDP-Gal onto the xyloside acceptor, we first synthesized a 4-deoxy derivative of 4-MUX (4H-Xyl-MU, Fig. 4A) and tested this compound as inhibitor of h β 4GalT7 *in vitro*. 4H-Xyl-MU was able to inhibit up to 50% of the initial activity at a 2 mM concentration (Fig. 4B), with an IC₅₀ value of about 1 mM and a K_i value of about 0.5 mM (Table 2). To test whether hydrogen bond formation between 4-MUX and the protein *via* H195 is important for the inhibitory potency, we synthesized 4H-Xyl-NP which aglycone structure is unable to establish such interaction and compared its inhibitory effect to 4H-Xyl-MU. This compound produced a decrease of h β 4GalT7 activity towards 4-MUX less than 25% at the highest concentration (Fig. 4B) that did not

allow determining IC₅₀ and K_i values. These results clearly indicated that 4H-Xyl-NP is a weak inhibitor of h β 4GalT7. We next substituted the equatorial hydrogen of the C4 atom of the Xyl moiety by a fluorine atom, closer to oxygen in term of electronegativity and predicted to fit the active site in term of steric hindrance. 4F-Xyl-MU led to up to 60% inhibition of the h β 4GalT7 activity at the highest concentration (Fig. 4B), with an IC₅₀ of 0.06 mM and a K_i of 0.03 mM. The inhibition constant for this compound is more than ten-times lower than that reached for the deoxy-analog (Table 2).

To complement the *in vitro* assay, we assessed the ability of the synthesized xyloside derivatives to inhibit GAG chains biosynthesis *in cellulo*. Addition of 4H-Xyl-NP produced a moderate but significant 20% decrease of GAG chains synthesis in CHOpgsB-618 cells, when used at 50 and 100 μ M (Fig. 5A). This correlated with the weak *in vitro* inhibition level obtained with this compound. The compound 4H-Xyl-MU allowed a larger inhibition of GAG chains synthesis, with up to 30% reduction of the GAG synthesis rate at similar concentrations (Fig. 5B). The best inhibitory effect was observed when performed in the presence of 4F-Xyl-MU leading to up to 50% inhibition of the initial GAG chains synthesis rate at 100 μ M concentration (Fig. 5C). Interestingly, preliminary results indicated that 400 μ M of 4F-Xyl-MU inhibited the initial decorin glycosylation rate by about 50%, without affecting the viability of CHOpgsB-618 cells (data not shown). Altogether, the latter data confirmed that this fluorinated compound should be considered as a promising non-cytotoxic xyloside-based inhibitor of h β 4GalT7.

DISCUSSION

β 4GalT7 is a unique enzyme in the GAG biosynthetic pathway with regard to its capacity to use exogenous xyloside molecules as substrates and/or inhibitors that can efficiently modulate GAG synthesis *in vitro* and *in vivo* (19, 20, 45). This glycosyltransferase is also central in the GAG synthesis process since the formation of the tetrasaccharide linker is a prerequisite to the polymerization of both HS and CS/DS chains. The human enzyme thus represents a prime target for the design of effectors of GAG synthesis as drugs to correct GAG disorders associated with numerous malignant conditions such as genetic diseases and cancer. To meet this challenge, we pioneered structure-function studies of the recombinant h β 4GalT7. We previously carried out structural, thermodynamical and phylogenetic investigations that identified key amino acid residues mainly implicated in the recognition and binding of the

donor substrate (31, 46). We also provided insight into the molecular basis of the GAG defects characterizing rare forms of EDS syndrome (17, 47). In the present work, in order to develop xyloside compounds that will specifically target the h β 4GalT7 activity for therapeutic purpose, we explored the architecture of the acceptor substrate binding site. To this aim, we combined functional investigations including site-directed mutagenesis, kinetic analyses, *in vitro* and *in cellulo* evaluation of galactosyltransferase activity and GAG synthesis, and a computational approach. This allowed mapping the acceptor binding site and to design and synthesize a potent xyloside-based inhibitor of GAG synthesis.

We first targeted a set of three tyrosine residues Y194, Y196 and Y199, as well as H195 belonging to the same conserved motif, that occupy a strategic position surrounding the xyloside acceptor substrate (34 and present data). Our mutational analysis led to a remarkable observation since alanine substitution of each of these tyrosine completely abolished h β 4GalT7 activity. The tyrosine-alanine mutants *i*) were devoid of galactosyltransferase activity *in vitro*, *ii*) were unable to prime GAG synthesis from 4-MUX *in cellulo*, *iii*) did not promote decorin glycosylation, thus supporting a prominent function of this set of aromatic residues. Mutating Y194, Y196 and Y199 with phenylalanine, revealed that the substitution differently affected h β 4GalT7 activity depending on the position. Noteworthy, the presence of the hydroxyl group of Y194 was indispensable since the conservative Y194F mutant completely lacked *in vitro* or *in cellulo* galactosyltransferase activity towards 4-MUX and was unable to sustain glycosylation of decorin. This observation is likely to be explained by a functionally important interaction between the hydroxyl group of this tyrosine and the β -phosphoryl group of UDP-Gal that was observed in all structures and models of β 4GalT7 (34 and this report, see Fig. 1). Most importantly, our computational model and experimental data suggested that the critical role of Y194 also arises from a stacking interaction between the aromatic ring of this residue and the 4-methylumbelliferyl moiety of 4-MUX. Altogether, these data indicate that Y194 occupies a strategic location in the catalytic center and interacts with both the donor nucleotide and the aglycone group of 4-MUX. In the case of Y196, the presence of the hydroxyl group of the tyrosine residue was also a major structural element since its replacement by phenylalanine only slightly restored the activity towards 4-MUX *in vitro* and *in cellulo*. The Y196F mutant did not sustain decorin glycosylation, also supporting an important role of this residue in the glycosylation of

endogenous proteoglycans. Our model provides a molecular explanation to these results, since it shows that Y196 is not directly involved in the binding of the acceptor substrate but rather forms a hydrogen-bond between its hydroxyl group and D229, this latter residue establishing an important interaction with O2 of the Xyl moiety. This supports the idea that interactions with the hydroxyl in C2 position control a strict geometry *via* both D229 and Y196, in agreement with the physiologically important regulatory role of Xyl-phosphate substitution in position 2 on GAG synthesis (41, 48). Furthermore, our model suggests that this residue is part of the cavity floor in agreement with structural data indicating that the acceptor substrate xylobiose is located in a hydrophobic binding pocket formed by Y177, Y179 and W207 in the *Drosophila* structure, and by Y194, Y196 and W224 in h β 4GalT7. The present data complements our previous findings demonstrating that W224 is a crucial active site residue (31). Differently to the preceding studied tyrosines, h β 4GalT7 well tolerated the substitution of tyrosine to phenylalanine at position 199 leading to a mutant that was active towards 4-MUX *in vitro* and was able to prime GAG synthesis from 4-MUX and onto decorin core protein. Consistently, Y199 is substituted by a phenylalanine in the *Drosophila* enzyme, suggesting that the presence of a hydrophobic aromatic ring is sufficient at this position. Further analysis of our molecular model predicts hydrogen bond formation between the tyrosine hydroxyl group of Y199 and O2 of the Gal moiety of UDP-Gal. However, no significant change in the K_m value towards UDP-Gal was observed for the Y199F mutant, indicating that this interaction may not play a critical functional role in nucleotide binding. The location of Y199 favors a role as contributor to the hydrophobic surrounding of the acceptor substrate binding pocket together with Y194, Y196 and W224 residues when h β 4GalT7 is in its closed conformation (34).

Investigation of the structural role of H195 led to most interesting findings for the design of efficient substrates and inhibitors of h β 4GalT7. We predicted that the nitrogen atom of the peptide backbone of this residue forms a hydrogen-bond with the carbonyl group of the coumarin moiety of 4-MUX. This is in full agreement with our mutational study that showed no major effect upon changing the side-chain of the histidine residue at this position by alanine, glutamine or arginine substitution on h β 4GalT7 activity monitored *in vitro* and *in cellulo*. However, the functional importance of an interaction between H195 backbone and 4-MUX was clearly emphasized by the stronger inhibitory effect of 4-deoxy-Xyl-MU compared to 4-deoxy-

Xyl-NP. We also found that 4-MUX was used as a substrate with a better affinity than Xyl-NP (data not shown). Noteworthy, among a series of naphthyl-xylosides, Siegbahn *et al.* (29) showed that 6-hydroxy-naphthyl-Xyl was able to prime GAG chains more efficiently than any other unsubstituted derivative in breast cancer cell lines. Altogether, this gives strong evidence that H195 through its backbone provides an important structural element for efficient binding of 4-MUX derivatives, and offers a molecular explanation for the superiority of 4-MUX synthesized in this study over naphthyl and benzyl-substituted xylosides previously reported in the literature (25, 30).

We also discovered a unique active site basic residue *i.e.* R226. Interestingly, this residue is located between the aromatic-rich ²²¹FWGWG²²⁵ sequence, containing W224 that interacts with the β -phosphate O-atom of the donor substrate, and the ²²⁷EDDE²³⁰ sequence containing acidic residues that are involved in Xyl binding and in the transfer reaction (31). Our functional analysis showed that modifying the side chain of R226 by site-directed mutagenesis did not affect the enzyme affinity towards acceptor or donor substrate. This is in line with the computational analysis indicating that the nitrogen atom of the peptide backbone of R226, but not its side-chain, interacts with the O3 atom of the Xyl moiety. Figures 1A and 1B clearly show that this residue, together with W224, are brought close to the aromatic triad in the closed conformation of h β 4GalT7.

We also investigated the role of R270 which substitution by a cysteine residue is implicated in the progeroid form of EDS (49). Our previous studies revealed that this genetic mutation dropped *in vitro* h β 4GalT7 activity and impaired GAG chains synthesis in CHO-pgsB618 cells (17). These effects were suggested to be due to a loss of hydrogen-bonding between the lateral chain of R270 and the hydroxyl group of a serine residue from PG core protein (17). This idea was supported by later molecular modeling indicating that R270 borders the catalytic site of h β 4GalT7 in the closed conformation (34 and this work, see Fig. 1A). However, the precise mechanism by which R270 modulates *in vitro* and *ex vivo* h β 4GalT7 activities remains unclear. Indeed, current crystal structures and molecular models do not point to a specific role of this residue in catalysis or substrate binding, consistent with kinetic data showing that mutations of R270 in alanine and lysine moderately affect h β 4GalT7 activity and affinity, and the observation that in *Drosophila*, the corresponding position is occupied by a lysine residue. The R270 residue is located in the flexible loop [261-284] that moves upon donor substrate binding, thus creating the

acceptor substrate binding site. This conformational change leads to the closed and catalytically competent conformation of the active site. It thus can be expected that any mutations affecting the loop movement would impair the transfer reaction. However, why the substitution of R270 by a cysteine residue, that causes the progeroid form of EDS patients, produces more deleterious consequences than alanine or lysine mutations requires further investigation of the conformational modifications operating during the catalytic cycle.

Our current and previous functional and computational approaches provide a detailed cartography of the h β 4GalT7 acceptor substrate binding pocket for the rational design of xyloside-based inhibitors (31). We show that the active site organization is governed, on one side, by a series of aromatic amino acids comprising three Tyr residues *i.e.* Y194, Y196 and Y199, which together with W224 create a hydrophobic environment and provide stacking interactions essential to the binding of both the xylosyl and aglycone parts of the acceptor substrate. On the opposite side of the site, it involves a network of hydrogen-bonding interactions between three charged amino acids *i.e.* D228, D229 and R226 and the hydroxyl groups of the Xyl moiety and other active site residues. Until now, most studies aiming to inhibit cellular and extracellular GAG synthesis have been targeted to the synthesis and testing of xyloside derivatives acting as substrates of β 4GalT7 thus reducing the glycosylation of endogenous proteoglycan core proteins (19). This approach successfully provided promising pharmacological agents, in particular anti-tumor compounds (45, 50). However, since such molecules behave both as exogenous primers of GAG synthesis and inhibitors of endogenous GAG formation, deciphering their mechanism of action remains challenging. With the perspective of designing xyloside derivatives that selectively act as inhibitors of GAG formation, we opted for C4-modified analogs, whose modification at C4 position prevents the catalytic transfer, and first synthesized deoxy-derivatives. In addition, we took advantage of the information gained from our structural and mutational analyses. We considered two key elements of the aglycone binding *i.e.* the strategic position of Y194 that forms stacking interactions with the aglycone part of the acceptor substrate as well as the interaction between H195 N-backbone and the carbonyl group of the coumarinyl moiety. In agreement with our prediction, our results clearly show that the 4-deoxy-xyloside appended to 4-MU was superior to the naphthyl-substituted molecule, as indicated by *in vitro* and *in cellulo* studies, supporting the idea that the hydrogen-bond between H195 and the carbonyl

group of the coumaryl group is crucial. Interestingly, Tsuzuki *et al.* (28) found that among triazole-xyloside derivatives generated by click chemistry bearing various aromatic and non aromatic aglycones, the *p*-nitrophenyl analog was the best inhibitor of PG synthesis when screened in endothelial cells. Although detailed docking of these triazole derivatives should be performed, it is tempting to speculate that the formation of a hydrogen bond interaction between the aglycone nitro group and H195 enhances the inhibitory potential compared to the other substituted benzyl derivatives. Furthermore, we show here that the 4-deoxy-4-fluorinated-4-MUX was superior to the unsubstituted 4-deoxy-analog, indicating that addition of an electronegative atom at this position is an important element in the design of potent inhibitors. The 4-hydroxyl group is involved in two hydrogen bonds with the carboxyl group of D228 and the 4-hydroxyl group of Gal, respectively. The replacement of the hydrogen-donor hydroxyl group by a fluorine atom that is larger than hydrogen and which van der Waals radius and electronegativity

are closer to oxygen, at the C4 position, enhanced binding interactions with h β 4GalT7. This corroborated previous studies showing that several fluorinated xylosides act as “good” substrate or inhibitor of GAG synthesis (18, 29, 30). In the same way, fluorinated thrombin inhibitors showed improved factor Xa binding (51). Further docking calculations of fluoro-substituted xylosides are underway to assess the mechanism underlying the improved interactive properties upon fluorine incorporation.

In summary, we developed a powerful approach for the design of xyloside inhibitors that specifically target h β 4GalT7. By integrating structural elements important for the binding of both the Xyl moiety and the hydrophobic aglycone, we synthesized a xyloside-based inhibitor of h β 4GalT7. We generated a compound that both impact *in vitro* galactosyltransferase activity and affect GAG synthesis in cells, opening promises for pharmacological applications. This molecule also represents a valuable chemical biology tool to explore the biological effects of GAGs.

REFERENCES

- Bernfield, M., Götte M., Park, P.W., Reizes, O., Fitzgerald, M.L., Lincecum, J., and Zako, M. (1999) Functions of cell surface heparan sulfate proteoglycans. *Annu. Rev. Biochem.* **68**, 729–777
- Clark, S. J., Bishop, P. N. and Day, A. J. (2013) The proteoglycan glycomatrix: a sugar microenvironment essential for complement regulation. *Front. Immunol.* **4**, 412
- Afratis, N., Gialeli, C., Nikitovic, D., Tseganidis, T., Karousou, E., Theocharis, A.D., Pavão, M.S., Tzanakakis, G.N., and Karamanos, N.K. (2012) Glycosaminoglycans: key players in cancer cell biology and treatment. *FEBS J.* **279**, 1177–1197
- Halper, J. (2014) Proteoglycans and diseases of soft tissues. *Adv. Exp. Med. Biol.* **802**, 49–58
- Wang, P., and Ding, K. (2014) Proteoglycans and glycosaminoglycans in misfolded proteins formation in Alzheimer’s disease. *Protein Pept. Lett.* **21**, 1048-1056
- Kadomatsu, K., and Sakamoto, K. (2014) Mechanisms of axon regeneration and its inhibition: roles of sulfated glycans. *Arch. Biochem. Biophys.* **558**, 36–41
- Sugahara, K., and Kitagawa, H. (2000) Recent advances in the study of the biosynthesis and functions of sulfated glycosaminoglycans. *Curr. Opin. Struct. Biol.* **10**, 518–527
- Yada, T., Gotoh, M., Sato, T., Shionyu, M., Go, M., Kaseyama, H., Iwasaki, H., Kikuchi, N., Kwon, Y.D., Togayachi, A., Kudo, T., Watanabe, H., Narimatsu, H., and Kimata, K. (2003) Chondroitin sulfate synthase-2. Molecular cloning and characterization of a novel human glycosyltransferase homologous to chondroitin sulfate glucuronyltransferase, which has dual enzymatic activities. *J. Biol. Chem.* **278**, 30235–30247
- Lind, T., Tufaro, F., McCormick, C., Lindahl, U., and Lidholt, K. (1998) The putative tumor suppressors EXT1 and EXT2 are glycosyltransferases required for the biosynthesis of heparan sulfate. *J. Biol. Chem.* **273**, 26265–26268
- Sheng, J., Xu, Y., Dulaney, S. B., Huang, X., and Liu, J. (2012) Uncovering biphasic catalytic mode of C5-epimerase in heparan sulfate biosynthesis. *J. Biol. Chem.* **287**, 20996–21002
- Honke, K., and Taniguchi, N. (2002) Sulfotransferases and sulfated oligosaccharides. *Med. Res. Rev.* **22**, 637–654
- Almeida, R., Levery, S.B., Mandel, U., Kresse, H., Schwientek, T., Bennett, E.P., and Clausen, H. (1999) Cloning and expression of a proteoglycan UDP-galactose: β -xylose β 1,4-galactosyltransferase I. A seventh member of the human β 4-galactosyltransferase gene family. *J. Biol. Chem.* **274**, 26165–26171
- Götte, M., Spillmann, D., Yip, G.W., Versteeg, E., Echtermeyer, F.G., van Kuppevelt, T.H., and Kiesel, L. (2008) Changes in heparan sulfate are associated with delayed wound repair, altered cell migration,

- adhesion and contractility in the galactosyltransferase I (beta4GalT-7) deficient form of Ehlers-Danlos syndrome. *Hum. Mol. Genet.* **17**, 996–1009
14. Okajima, T., Yoshida, K., Kondo, T., and Furukawa, K. (1999) Human homolog of *Caenorhabditis elegans* sqv-3 gene is galactosyltransferase I involved in the biosynthesis of the glycosaminoglycan-protein linkage region of proteoglycans. *J. Biol. Chem.* **274**, 22915–22918
 15. Furukawa, K., and Okajima, T. (2002) Galactosyltransferase I is a gene responsible for progeroid variant of Ehlers-Danlos syndrome: molecular cloning and identification of mutations. *Biochim. Biophys. Acta* **1573**, 377–381
 16. Götte, M., and Kresse, H. (2005) Defective glycosaminoglycan substitution of decorin in a patient with progeroid syndrome is a direct consequence of two point mutations in the galactosyltransferase I (beta4GalT-7) gene. *Biochem. Genet.* **43**, 65–77
 17. Bui, C., Talhaoui, I., Chabel, M., Mulliert, G., Coughtrie, M.W., Ouzzine, M., and Fournel-Gigleux, S. (2010) Molecular characterization of β 1,4-galactosyltransferase 7 genetic mutations linked to the progeroid form of Ehlers-Danlos syndrome (EDS). *FEBS Lett.* **584**, 3962–3968
 18. Lugemwa, F. N., Sarkar, A. K., and Esko, J. D. (1996) Unusual beta-D-xylosides that prime glycosaminoglycans in animal cells. *J. Biol. Chem.* **271**, 19159–19165
 19. Esko, J.D., Weinke, J.L., Taylor, W.H., Ekborg, G., Rodén, L., Anantharamaiah, G., and Gawish, A. (1987) Inhibition of chondroitin and heparan sulfate biosynthesis in Chinese hamster ovary cell mutants defective in galactosyltransferase I. *J. Biol. Chem.* **262**, 12189–12195
 20. Muto, J., Naidu, N.N., Yamasaki, K., Pineau, N., Breton, L., and Gallo, R.L. (2011) Exogenous addition of a C-xylopyranoside derivative stimulates keratinocyte dermatan sulfate synthesis and promotes migration. *PloS One* **6**, e25480
 21. Nguyen, T.K., Tran, V.M., Sorna, V., Eriksson, I., Kojima, A., Koketsu, M., Loganathan, D., Kjellén, L., Dorsky, R.I., Chien, C.B., and Kuberan, B. (2013) Dimerized glycosaminoglycan chains increase FGF signaling during zebrafish development. *ACS Chem. Biol.* **8**, 939–948
 22. Martin, N.B., Masson, P., Sepulchre, C., Theveniaux, J., Millet, J., and Bellamy, F. (1996) Pharmacologic and biochemical profiles of new venous antithrombotic beta-D-xyloside derivatives: potential antiathero/thrombotic drugs. *Semin. Thromb. Hemost.* **22**, 247–254
 23. Vassal-Stermann, E., Duranton, A., Black, A.F., Azadiguian, G., Demaude, J., Lortat-Jacob, H., Breton, L., and Vivès, R.R. (2012) A New C-Xyloside induces modifications of GAG expression, structure and functional properties. *PloS One* **7**, e47933
 24. Raman, K., Ninomiya, M., Nguyen, T.K., Tsuzuki, Y., Koketsu, M., and Kuberan, B. (2011) Novel glycosaminoglycan biosynthetic inhibitors affect tumor-associated angiogenesis. *Biochem. Biophys. Res. Commun.* **404**, 86–89
 25. Mani, K., Havsmark, B., Persson, S., Kaneda, Y., Yamamoto, H., Sakurai, K., Ashikari, S., Habuchi, H., Suzuki, S., Kimata, K., Malmström, A., Westergren-Thorsson, G., and Fransson, L.A. (1998) Heparan/chondroitin/dermatan sulfate primer 2-(6-hydroxynaphthyl)-O- β -D-xylopyranoside preferentially inhibits growth of transformed cells. *Cancer Res.* **58**, 1099–1104
 26. Kolset, S. O., Sakurai, K., Ivhed, I., Overvatn, A., and Suzuki, S. (1990) The effect of β -D-xylosides on the proliferation and proteoglycan biosynthesis of monoblastic U-937 cells. *Biochem. J.* **265**, 637–645
 27. Garud, D. R., Tran, V. M., Victor, X. V., Koketsu, M. and Kuberan, B. (2008) Inhibition of heparan sulfate and chondroitin sulfate proteoglycan biosynthesis. *J. Biol. Chem.* **283**, 28881–28887
 28. Tsuzuki, Y., Nguyen, T. K. N., Garud, D. R., Kuberan, B., and Koketsu, M. (2010) 4-deoxy-4-fluoroxyloside derivatives as inhibitors of glycosaminoglycan biosynthesis. *Bioorg. Med. Chem. Lett.* **20**, 7269–7273
 29. Siegbahn, A., Aili, U., Ochocinska, A., Olofsson, M., Rönnols, J., Mani, K., Widmalm, G., and Ellervik, U. (2011) Synthesis, conformation and biology of naphthoxylosides. *Bioorg. Med. Chem.* **19**, 4114–4126
 30. Siegbahn, A., Manner, S., Persson, A., Tykesson, E., Holmqvist, K., Ochocinska, A., Rönnols, J., Sundin, A., Mani, K., Westergren-Thorsson, G., Widmalm, G., and Ellervik, U. (2014) Rules for priming and inhibition of glycosaminoglycan biosynthesis; probing the β 4GalT7 active site. *Chem. Sci.* **5**, 3501–3508
 31. Talhaoui, I., Bui, C., Oriol, R., Mulliert, G., Gulberti, S., Netter, P., Coughtrie, M.W., Ouzzine, M., and Fournel-Gigleux, S. (2010) Identification of key functional residues in the active site of human β 1,4-galactosyltransferase 7: a major enzyme in the glycosaminoglycan synthesis pathway. *J. Biol. Chem.* **285**, 37342–37358
 32. Rahuel-Clermont, S., Daligault, F., Piet, M.H., Gulberti, S., Netter, P., Branlant, G., Magdalou, J., and Lattard, V. (2010) Biochemical and thermodynamic characterization of mutated β 1,4-galactosyltransferase 7 involved in the progeroid form of the Ehlers-Danlos syndrome. *Biochem. J.* **432**,

33. Ramakrishnan, B., and Qasba, P. K. (2010) Crystal structure of the catalytic domain of *Drosophila* β 1,4-Galactosyltransferase-7. *J. Biol. Chem.* **285**, 15619–15626
34. Tsutsui, Y., Ramakrishnan, B., and Qasba, P. K. (2013) Crystal structures of β -1,4-galactosyltransferase 7 enzyme reveal conformational changes and substrate binding. *J. Biol. Chem.* **288**, 31963–31970
35. Eneyskaya, E.V., Ivanen, D.R., Shabalin, K.A., Kulminskaya, A.A., Backinowsky, L.V., Brumer, I.H., and Neustroev, K.N. (2005) Chemo-enzymatic synthesis of 4-methylumbelliferyl β -(1 \rightarrow 4)-D-xylooligosides: new substrates for β -D-xylanase assays. *Org. Biomol. Chem.* **3**, 146–151
36. Sastry, G. M., Adzhigirey, M., Day, T., Annabhimoju, R., and Sherman, W. (2013) Protein and ligand preparation: parameters, protocols, and influence on virtual screening enrichments. *J. Comput. Aided Mol. Des.* **27**, 221–234
37. Kaminski, G. A., Friesner, R. A., Tirado-Rives, J., and Jorgensen, W. L. (2001) Evaluation and reparametrization of the OPLS-AA Force field for proteins via comparison with accurate quantum chemical calculations on peptides. *J. Phys. Chem. B* **105**, 6474–6487
38. Banks, J.L., Beard, H.S., Cao, Y., Cho, A.E., Damm, W., Farid, R., Felts, A.K., Halgren, T.A., Mainz, D.T., Maple, J.R., Murphy, R., Philipp, D.M., Repasky, M.P., Zhang, L.Y., Berne, B.J., Friesner, R.A., Gallicchio, E., and Levy, R.M. (2005) Integrated Modeling Program, Applied Chemical Theory (IMPACT). *J. Comput. Chem.* **26**, 1752–1780
39. Friesner, R.A., Banks, J.L., Murphy, R.B., Halgren, T.A., Klicic, J.J., Mainz, D.T., Repasky, M.P., Knoll, E.H., Shelley, M., Perry, J.K., Shaw, D.E., Francis, P., and Shenkin, P.S. (2004) Glide: a new approach for rapid, accurate docking and scoring. 1. Method and assessment of docking accuracy. *J. Med. Chem.* **47**, 1739–1749
40. Repasky, M. P., Shelley, M., and Friesner, R. A. (2007) Flexible ligand docking with Glide. *Curr. Protoc. Bioinforma. Ed. Board Andreas Baxevanis Al Chapter 8*, Unit 8.12
41. Gulberti, S., Lattard, V., Fondeur, M., Jacquinet, J.C., Mulliert, G., Netter, P., Magdalou, J., Ouzzine, M., and Fournel-Gigleux, S. (2005) Phosphorylation and sulfation of oligosaccharide substrates critically influence the activity of human β 1,4-galactosyltransferase 7 (GalT-I) and β 1,3-glucuronosyltransferase I (GlcAT-I) involved in the biosynthesis of the glycosaminoglycan-protein linkage region of proteoglycans. *J. Biol. Chem.* **280**, 1417–1425
42. Cheng, Y., and Prusoff, W. H. (1973) Relationship between the inhibition constant (K₁) and the concentration of inhibitor which causes 50 per cent inhibition (I₅₀) of an enzymatic reaction. *Biochem. Pharmacol.* **22**, 3099–3108
43. Lazareno, S., and Birdsall, N. J. (1993) Estimation of competitive antagonist affinity from functional inhibition curves using the Gaddum, Schild and Cheng-Prusoff equations. *Br. J. Pharmacol.* **109**, 1110–1119
44. Fournel-Gigleux, S., Jackson, M. R., Wooster, R., and Burchell, B. (1989) Expression of a human liver cDNA encoding a UDP-glucuronosyltransferase catalysing the glucuronidation of hyodeoxycholic acid in cell culture. *FEBS Lett.* **243**, 119–122
45. Belting, M., Borsig, L., Fuster, M.M., Brown, J.R., Persson, L., Fransson, L.A., and Esko, J.D. (2002) Tumor attenuation by combined heparan sulfate and polyamine depletion. *Proc. Natl. Acad. Sci. U. S. A.* **99**, 371–376
46. Daligault, F., Rahuel-Clermont, S., Gulberti, S., Cung, M.T., Branlant, G., Netter, P., Magdalou, J., Lattard, V. (2009) Thermodynamic insights into the structural basis governing the donor substrate recognition by human β 1,4-galactosyltransferase 7. *Biochem. J.* **418**, 605–614
47. Malfait, F., Kariminejad, A., Van Damme, T., Gauche, C., Syx, D., Merhi-Soussi, F., Gulberti, S., Symoens, S., Vanhauwaert, S., Willaert, A., Bozorgmehr, B., Kariminejad, M.H., Ebrahimiadib, N., Hausser, I., Huysseune, A., Fournel-Gigleux, S., and De Paepe, A. (2013) Defective initiation of glycosaminoglycan synthesis due to *B3GALT6* mutations causes a pleiotropic Ehlers-Danlos-syndrome-like connective tissue disorder. *Am. J. Hum. Genet.* **92**, 935–945
48. Ueno, M., Yamada, S., Zako, M., Bernfield, M., and Sugahara, K. (2001) Structural characterization of heparan sulfate and chondroitin sulfate of syndecan-1 purified from normal murine mammary gland epithelial cells. Common phosphorylation of xylose and differential sulfation of galactose in the protein linkage region tetrasaccharide sequence. *J. Biol. Chem.* **276**, 29134–29140
49. Seidler, D.G., Faiyaz-UI-Haque, M., Hansen, U., Yip, G.W., Zaidi, S.H., Teebi, A.S., Kiesel, L., and Götte, M. (2006) Defective glycosylation of decorin and biglycan, altered collagen structure, and abnormal phenotype of the skin fibroblasts of an Ehlers-Danlos syndrome patient carrying the novel Arg270Cys substitution in galactosyltransferase I (β 4GalT-7). *J. Mol. Med. Berl. Ger.* **84**, 583–594
50. Mani, K., Belting, M., Ellervik, U., Falk, N., Svensson, G., Sandgren, S., Cheng, F., and Fransson, L.A. (2004) Tumor attenuation by 2(6-hydroxynaphthyl)- β -D-xylopyranoside requires priming of heparan

sulfate and nuclear targeting of the products. *Glycobiology* **14**, 387–397

51. Hagmann, W. K. (2008) The many roles for fluorine in medicinal chemistry. *J. Med. Chem.* **51**, 4359–4369

FOOTNOTES

¹ This work was supported by Agence Nationale pour la Recherche (ANR) Meca-GT (Grant ANR-13-BSV8-0011-01), ANR GAG-Sorting (Grant ANR-13-JS07-0004-01), Labex SynOrg (ANR-11-LABX-0029), International Associated Laboratory CNRS-Université de Lorraine - University of Dundee, *SFGEN*, Région Lorraine-FEDER (Glyco-Fluo) Grant, and grants from Région Lorraine to NR and to SFG. This work was also partially supported by the patient's association AMSEDgenetique (Mrs Valérie Gisclard is sincerely acknowledged for her profound implication). Miss Anne Robert is gratefully acknowledged for excellent technical assistance.

²CS, chondroitin sulfate ; DS, dermatan sulfate ; EDS, Ehlers-Danlos syndrome ; GAG, glycosaminoglycan ; Gal, galactose ; HS, heparan sulfate ; 4-MU, 4-methylumbelliferone ; NP, naphthyl ; PG, proteoglycan ; Xylose, Xyl.

FIGURE LEGENDS

FIGURE 1. Molecular modeling of h β 4GalT7 structure. A) View of the active-site of h β 4GalT7 in complex with donor (UDP-Gal) and acceptor (4-MUX) substrate. The protein α -carbon trace is represented as grey ribbons; the purple ribbon corresponds to the protein backbone that is not seen in the open conformation. B) Surface representation of the acceptor binding site, in the same orientation as in A. The electrostatic potential is mapped onto the protein surface and is colored from red (negative) to blue (positive).

FIGURE 2. Effect of wild-type and mutated h β 4GalT7 expression on GAG chains primed from 4-MUX in CHOpgsB-618 cells. Cells were transiently transfected with wild-type (WT) or mutated h β 4GalT7 cDNA or with empty vector (pcDNA), and GAG chains synthesis was quantified by scintillation counting following Na₂[³⁵SO₄²⁻] incorporation, using 0 (white bars), 5 (grey bars) and 10 μ M (black bars) 4-MUX. Immunoblot analyses of the protein expression level in CHOpgsB-618 cells transfected with the vector coding for the wild-type or mutated h β 4GalT7 are shown as insert. The enzyme was identified at the band of \sim 35 kDa, while the upper band corresponding to \sim 39 kDa band could be attributed to the *N*-glycosylated enzyme as demonstrated by its disappearance upon addition of PNGase F (*left panel*). Both bands intensities were used to quantify the total protein expression level (ImageJ software). The immunoblot analysis indicates that the mutated enzymes were all expressed at a comparable level to that of the wild-type h β 4GalT7 (*right panel*). Data are means \pm S.E. of three independent experiments performed in triplicate. Statistical analysis was carried out by the Student's *t*-test with *, $p < 0.05$, **, $p < 0.01$ and ***, $p < 0.001$ versus GAG synthesis in the absence of 4-MUX.

FIGURE 3. Effect of wild-type and mutated h β 4GalT7 expression on decorin core protein glycosylation in CHOpgsB-618 cells. Cells stably expressing the human recombinant decorin core protein were transfected with the recombinant vector encoding either the wild-type (WT) or mutated h β 4GalT7. The decorin glycosylation level was monitored by immunoblot then quantified using ImageJ software, as described in *Experimental Procedures*. Immunoblot analyses of the decorin core protein glycanation level are shown as inserts for CHOpgsB-618 cells transfected with empty (pcDNA) or with the recombinant vector coding for WT, Y194A, Y194F, Y196A, Y196F, Y199A or Y199F h β 4GalT7 (*left panel*), and for WT, R270A, R270K, R226A, R226K, H195A, H195Q, or H195R h β 4GalT7 (*right panel*). The band observed at a molecular mass of \sim 35 kDa can be attributed to the decorin core protein, while the wide upper band corresponding to a molecular mass \geq 75 kDa corresponds to the glycosylated decorin. Data are means \pm S.E. from three independent experiments performed in triplicate. Statistical analysis was carried out by the Student's *t*-test with **, $p < 0.01$ and ***, $p < 0.001$ versus decorin glycosylation in cells expressing the wild-type h β 4GalT7.

FIGURE 4. Inhibitory effect of C4-modified xylosides on h β 4GalT7 activity. A) Chemical structures of the xyloside analogs synthesized and tested as inhibitors. From left to right: 4H-Xyl-NP, 4H-Xyl-MU and 4F-Xyl-MU. B) Inhibition assays using purified recombinant wild-type h β 4GalT7 in the presence of fixed 4-MUX (0.5 mM) and UDP-Gal (1 mM). Activities are presented as function of the logarithm of increasing inhibitor concentrations (0-5 mM); (\blacktriangle) 4H-Xyl-NP, (\blacksquare) 4H-Xyl-MU, (\circ) 4F-Xyl-MU. Results are the means values \pm S.E. of three independent determinations on assays performed in duplicate.

FIGURE 5. Inhibitory effect of C4-modified xylosides upon 4-MUX-primed GAG chains synthesis in CHOpgsB-618 cells expressing the recombinant wild-type h β 4GalT7. CHOpgsB-618 cells transiently transfected with wild-type h β 4GalT7 cDNA were incubated with 5 μ M 4-MUX and Na₂[³⁵SO₄²⁻], in the presence of 4H-Xyl-NP (panel A) 4H-Xyl-MU (panel B) and 4F-Xyl-MU (panel C). The GAG expression level in cells transfected by the empty pcDNA vector was taken as negative control. Results are the means \pm S.E. of three independent experiments performed in triplicate. Statistical analysis was carried out using the Student's *t*-test with **, $p < 0.01$ and ***, $p < 0.001$ versus GAG synthesis rate in the absence of inhibitor.

TABLE 1.**Kinetic parameters of wild-type and mutant GST-β4GalT7**

Kinetic parameters towards donor (UDP-Gal) and acceptor (4-MUX) substrates were determined as described in *Experimental Procedures* section. The results are the mean values of three independent determinations ± S.D. on assays performed in duplicate. The results were analyzed with Student's *t*-test and considered as significant when $p < 0.05$ (*). ND indicates that no kinetic constant could be determined using excess acceptor or donor substrate.

Enzyme	k_{cat} (min ⁻¹)	UDP-Gal		4-MUX	
		K_m (mM)	k_{cat} / K_m (min ⁻¹ .mM ⁻¹)	K_m (mM)	k_{cat} / K_m (min ⁻¹ .mM ⁻¹)
GST-β4GalT7	90.5 ± 2.3	0.22 ± 0.02	425	0.35 ± 0.02	250
Y194A	ND	ND	-	ND	-
Y194F	ND	ND	-	ND	-
H195A	115.9 ± 9.7 *	0.40 ± 0.02 *	291	0.64 ± 0.02 *	180
H195Q	97.4 ± 2.4 *	0.33 ± 0.02 *	295	0.55 ± 0.02 *	177
H195R	89.6 ± 1.3	0.32 ± 0.02 *	295	0.35 ± 0.03	242
Y196A	ND	ND	-	ND	-
Y196F	30 ± 1.1 *	0.34 ± 0.06 *	88	1.06 ± 0.06 *	28
Y199A	ND	ND	-	ND	-
Y199F	72.3 ± 5.8 *	0.32 ± 0.02 *	243	0.59 ± 0.06 *	113
R226A	53.6 ± 2.0 *	0.34 ± 0.03 *	171	0.44 ± 0.05 *	112
R226K	81.1 ± 2.9 *	0.29 ± 0.02 *	282	0.46 ± 0.01 *	175
R270A	46.4 ± 0.2 *	0.27 ± 0.01 *	184	0.60 ± 0.02 *	72
R270K	48.7 ± 1.5 *	0.37 ± 0.02 *	139	0.54 ± 0.07 *	85

TABLE 2**Kinetic inhibition parameters of h β 4GalT7 with C4-modified xylosides**

IC₅₀ and K_i values are the mean values of three independent experiments \pm S.D. on assays performed in duplicate. ND, not determined.

Xylosides	IC₅₀ (mM)	K_i (mM)
4H-Xyl-NP	ND	ND
4H-Xyl-MU	1.28 \pm 0.22	0.53 \pm 0.10
4F-Xyl-MU	0.06 \pm 0.02	0.03 \pm 0.01

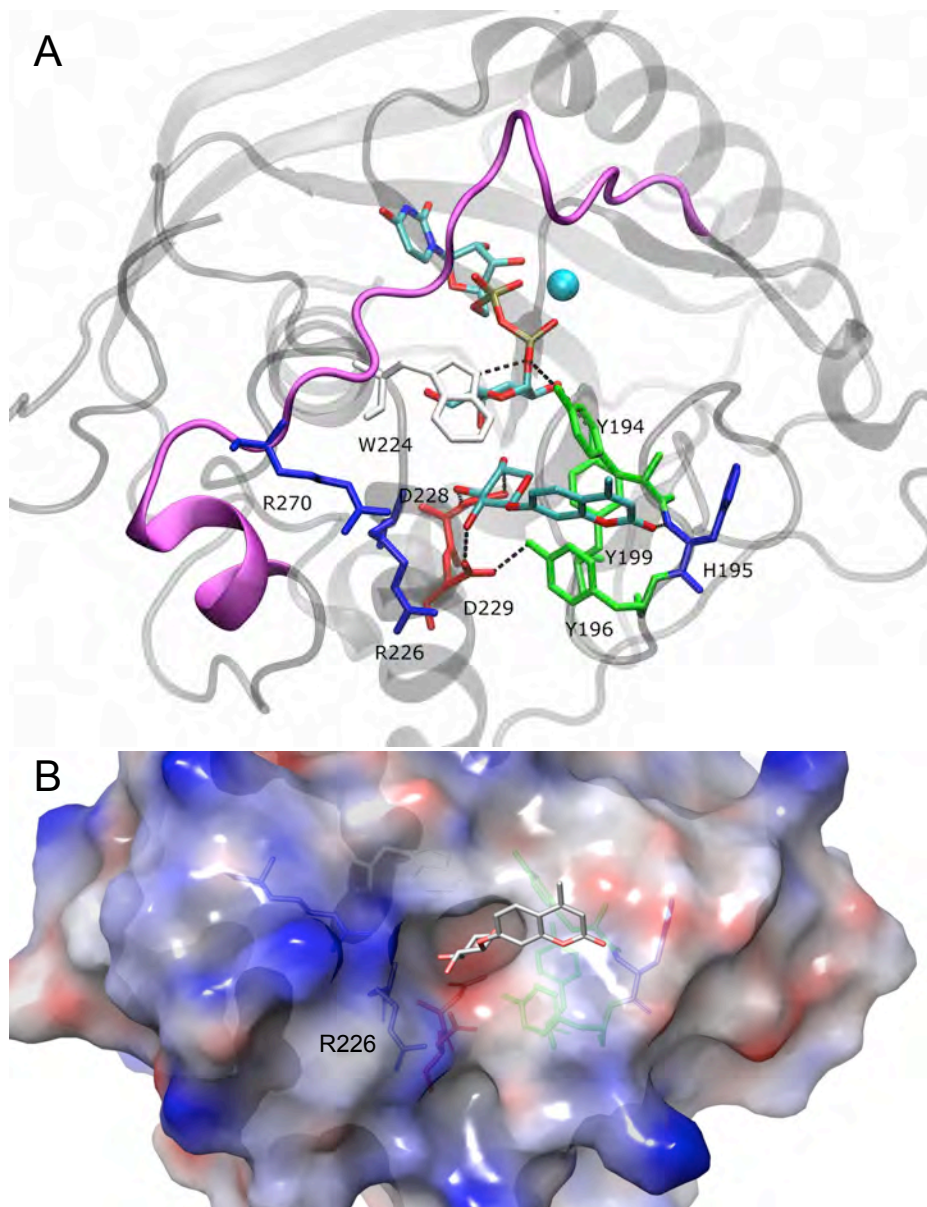
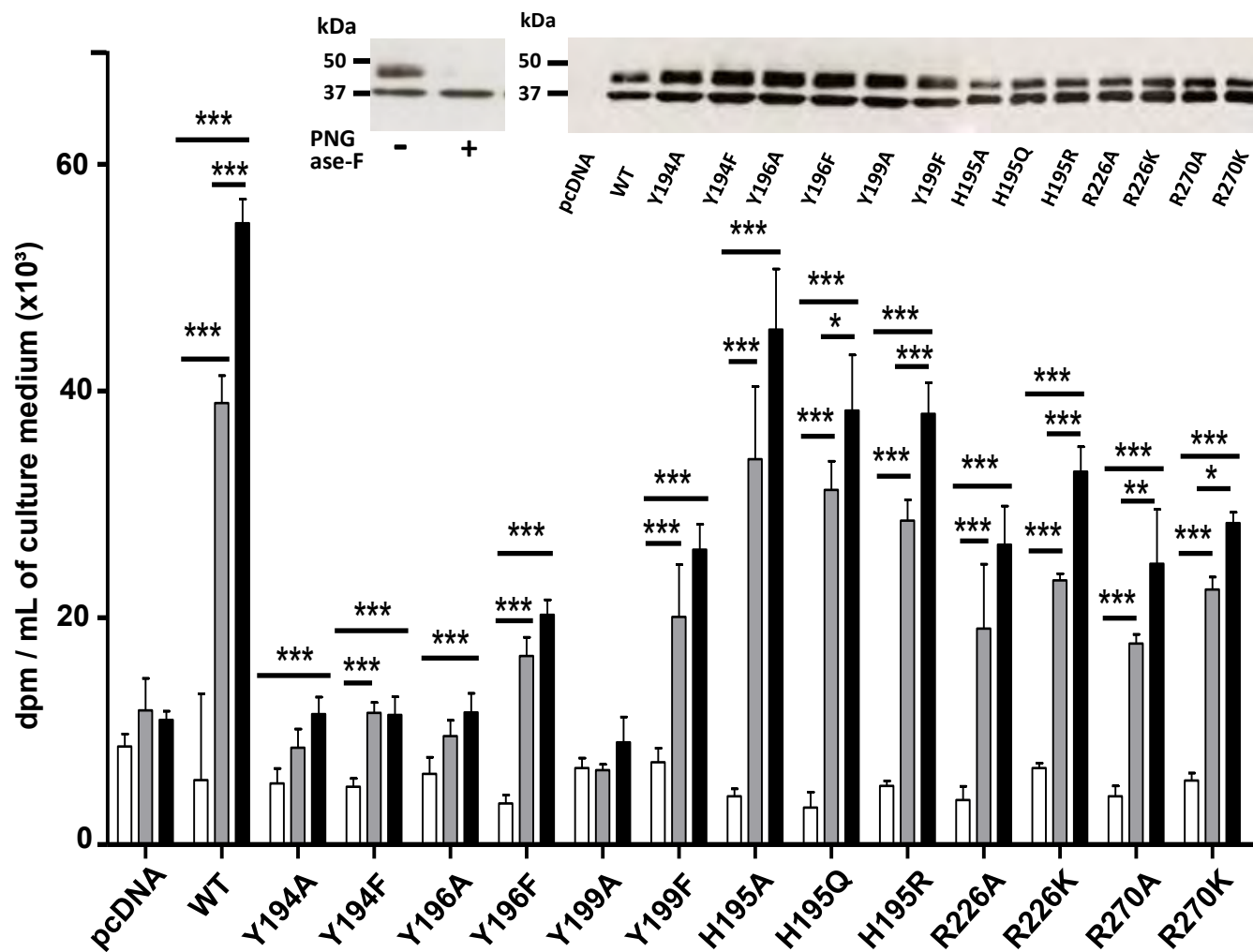
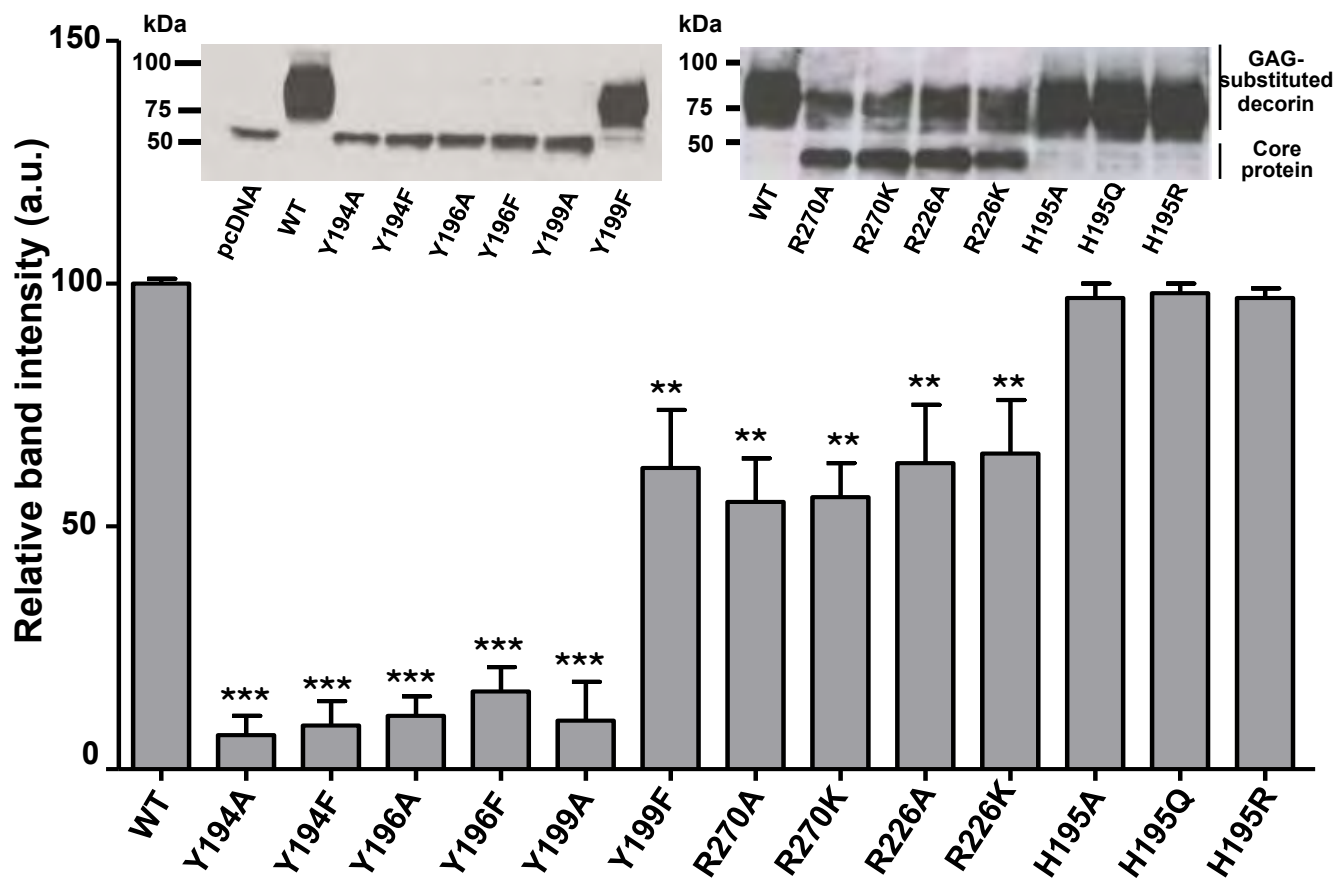
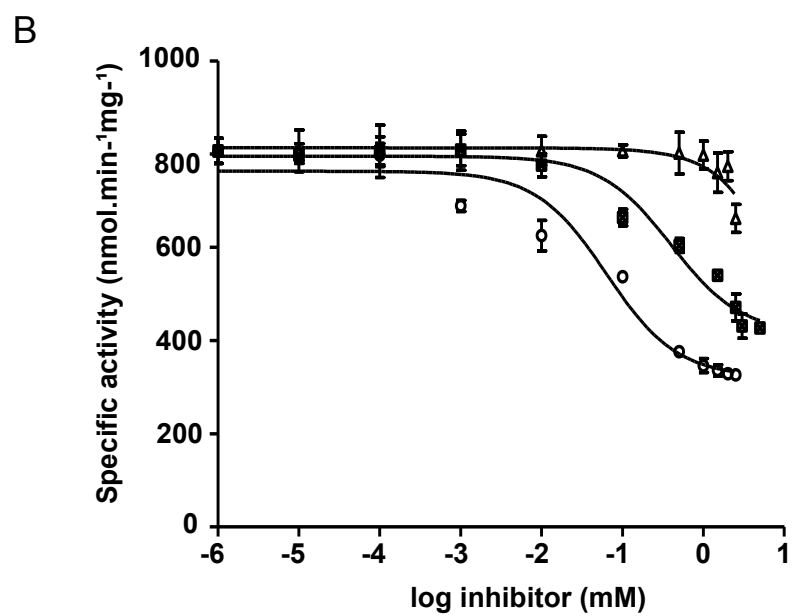
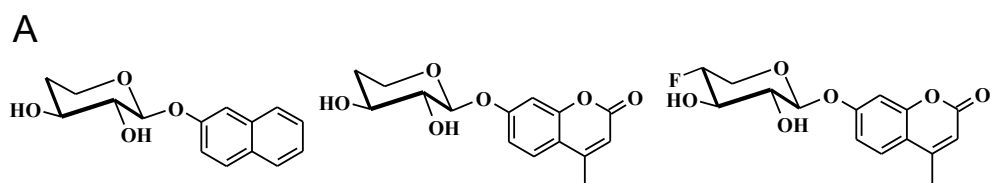
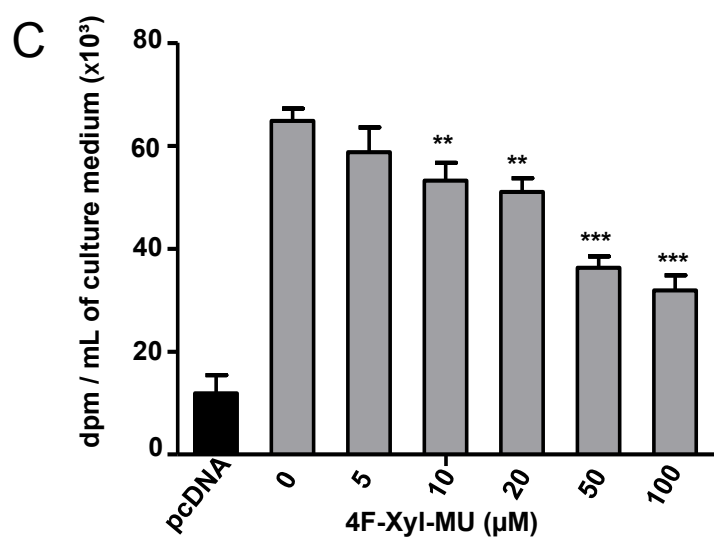
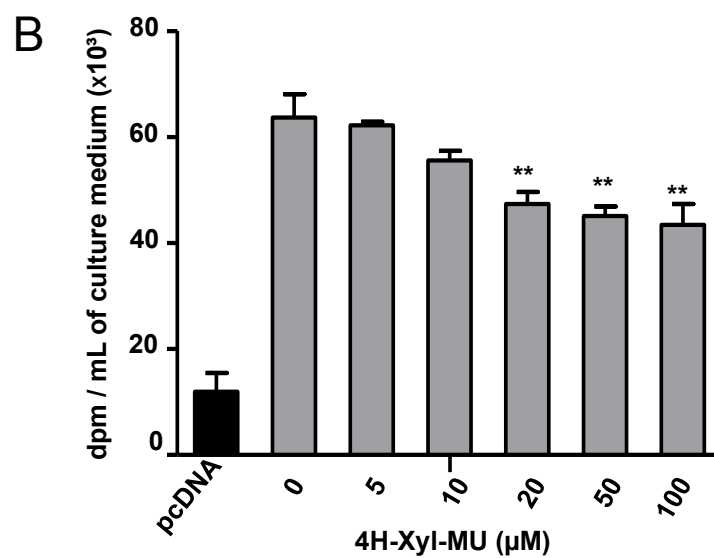
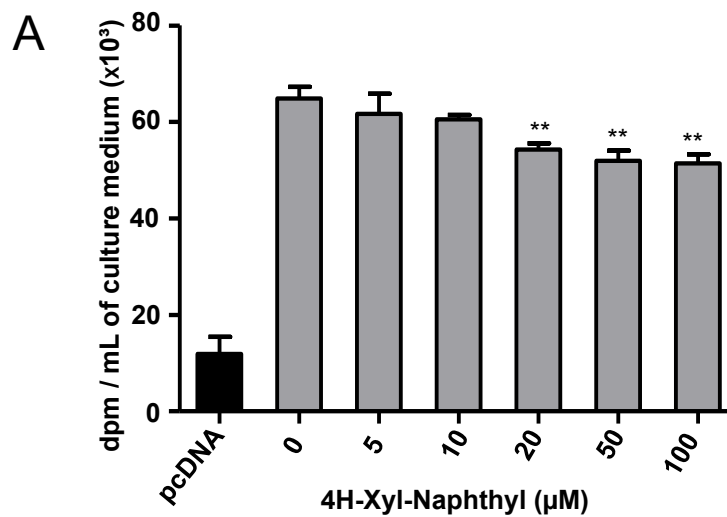


Figure 2









Glycobiology and Extracellular Matrices:
Probing the acceptor active site
organization of the human recombinant β
1,4-galactosyltransferase 7 and design of
xyloside-based inhibitors



Mineem Saliba, Nick Ramalanjaona, Sandrine
Gulberti, Isabelle Bertin-Jung, Aline Thomas,
Samir Dahbi, Chrystel Lopin-Bon,
Jean-Claude Jacquinet, Christelle Breton,
Mohamed Ouzzine and Sylvie
Fournel-Gigleux

J. Biol. Chem. published online January 7, 2015

Access the most updated version of this article at doi: [10.1074/jbc.M114.628123](https://doi.org/10.1074/jbc.M114.628123)

Find articles, minireviews, Reflections and Classics on similar topics on the [JBC Affinity Sites](#).

Alerts:

- [When this article is cited](#)
- [When a correction for this article is posted](#)

[Click here](#) to choose from all of JBC's e-mail alerts

This article cites 0 references, 0 of which can be accessed free at
<http://www.jbc.org/content/early/2015/01/07/jbc.M114.628123.full.html#ref-list-1>